Spectral Efficient Channel Estimation Algorithms for FBMC/OQAM Systems: A Comparison

Leonardo G. Baltar, Amine Mezghani, Josef A. Nossek
Institute for Circuit Theory and Signal Processing
Technische Universität München
80290 Munich, Germany
Email: leo.baltar@tum.de

***Abstract*—Spectrally efficient channel impulse response (CIR) estimation in the sense of minimal training overhead is a key issue for the successful deployment of Filter Bank Multicarrier (FBMC) with Offset Quadrature Amplitude Modulation (OQAM). In this contribution we perform a comparison between channel estimation algorithms considering two different models for the received subcarrier signals: a per-subcarrier narrowband and a broadband channel model. We also consider three cases of spectrally efficient channel estimation by employing different training sequence occupation of the subcarriers.**

I. Introduction

We consider FBMC systems in wireless environments with multipath propagation. In contrast to CP-OFDM, where a rectangular pulse shaping is used, we take a finite impulse response (FIR) prototype filter with a duration greater than the symbol period, but as in CP-OFDM it is modulated by complex exponentials. Consequently, more spectrally concentrated subcarriers are obtained which only overlap with the two adjacent ones. Moreover, the FBMC system does not include any guard interval (or CP), which also improves spectral efficiency, at the cost of higher complexity.

In FBMC, orthogonality, i.e. inter-symbol interference (ISI) and inter-channel interference (ICI)-free received symbols, can only be guaranteed by the so called OQAM, where the symbols' real and imaginary parts are staggered by $T/2$, and T is the QAM symbol period in each subcarrier [1]. Furthermore, the prototype filter can be designed according to different goals, but we restrict ourselves to an FIR approximation of the root raised cosine (RRC) with roll-off one. This choice of the prototype will indeed introduce some ISI and ICI, but if the filter degree is high enough, their is negligible compared to the other impairments, for example, ISI and ICI caused by the multipath channel or the thermal noise.

Channel estimation for FBMC/OQAM is currently an active area of research. In a typical multipath scenario the orthogonality inside one subcarrier and between adjacent subcarriers is lost. In current wireless communications standards that employ multicarrier modulation as LTE, for example, the training symbols used for channel estimation are typically distributed in the time-frequency plane and are also interleaved with data carrying symbols. In classical CP-OFDM, the use of such a training structure for channel estimation is straightforward, if the orthogonality between the subcarriers is guaranteed. In the case of FBMC/OQAM, since a fractionally spaced multi-tap channel exist in each subcarrier, the received signals are embedded not only in noise, but also in ISI and ICI interference with symbols transmitted in the vicinity of the training symbols.

One easy way to perform channel estimation free of all the interference terms is to transmit zeros around the training [2] or to fill three adjacent subcarriers with long training sequences [3]. To achieve maximum spectral efficiency by reducing the training overhead, a certain level of interference should be accepted by allowing data transmission in the subcarriers adjacent to the training subcarrier and/or using shorter training sequences to give more slots for data transmission.

In this contribution we will perform a performance comparison by considering three variants of interference embedded channel estimation. We call them estimation in the presence of ICI only, of ISI only and of both ICI and ISI. The results in this work can be further extended to consider algorithms like in [4] and [5] that improve the estimation performance in the presence of those interferences by iteratively estimating them.

In addition to that, we also compare two different models for the channel estimation in FBMC/OQAM. The first we call broadband based channel model, where the matrices are directly derived from the multirate system model of the OQAM/FBMC system. In the second framework, the narrowband based channel estimation [3], the idea is to write the model as a function of a narrowband channel for each subcarrier occupied with training. In both models the IR of the broadband channel is estimated and only the matrices used are different. Finally, the estimated CIR can be directly employed to calculate the linear equalizers of all subcarriers [6].

II. OQAM based Filter Bank Multicarrier Model

A high level model of the FBMC system is shown in Fig. 1. In this transmultiplex system, a synthesis filter bank (SFB) performs a frequency division multiplexing of the T seconds long QAM data symbols $d_k[m]$ at the transmitter. An analysis filter bank (AFB) at the receiver separates the data onto each subcarrier. We assume a slowly fading frequency selective channel. Usually M_u out of M subcarriers are used.

Here we regard exponentially modulated SFBs and AFBs, i.e. only one low-pass filter has to be designed and the other

978-1-4799-5863-4/14/$31.00 ©

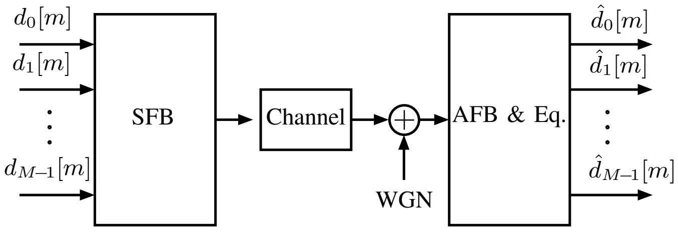

Figure 1. FBMC System Overview.

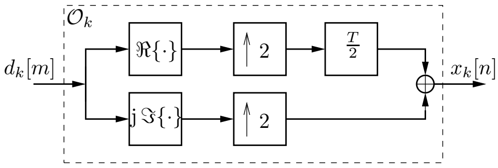

Figure 2. O-QAM staggering for odd indexed subcarrier

sub-filters are obtained by modulating it as follows [7]

$$g_k[l] = g_{\mathrm{P}}[l] \exp\left(\mathrm{j}\,\frac{2\pi}{M} k \left(l - \frac{L_{\mathrm{P}}-1}{2}\right)\right),\ l = 0, \ldots, L_{\mathrm{P}}-1,$$

where $g_{\mathrm{P}}[l]$ is the impulse response of this prototype filter of degree $L_{\mathrm{P}}-1$. The prototype chosen here is an RRC filter with roll-off factor one and consequently only the spectrum of contiguous subcarriers overlap. The non-contiguous subcarriers are separated by the high stop-band attenuation. We define $L_{\mathrm{P}} = KM + 1$, where K is the time overlapping factor that determines how many symbols superimpose. K should be kept as small as possible not only to limit the complexity but also to reduce the time-domain spreading of the symbols and the transmission latency.

To maintain the orthogonality between all subcarriers and for all time instants, the complex QAM input symbols $d_k[m]$ are OQAM staggered. We illustrate the OQAM staggering for odd indexed subcarriers in Fig. 2. For even indexed subcarriers the $T/2$ delay is placed at the lower branch. The OQAM de-staggering is performed at the receiver by the application of flow-graph reversal, substitution of up-samplers by down-samplers and exchange of $\Re\{\cdot\}$ and $\mathrm{j}\,\Im\{\cdot\}$.

After the OQAM staggering, the subcarrier signals are up-sampled by $M/2$, filtered and added. A broadband signal is then generated and digital-to-analog converted into an IQ baseband signal that is analog processed and transmitted. At the receiver side the RF signal is amplified, brought to baseband, filtered and then analog-to-digital converted. The received signal is then filtered and down-sampled by $M/2$.

The fact that only contiguous subcarriers overlap, allows us to construct the model for one subcarrier shown in Fig. 3. The inputs $x_k[n]$ are OQAM symbols and the received subcarrier signals $y_k[n]$ still have to be equalized and de-staggered before further processing of the QAM symbols. As a consequence, in this model the input and output sampling rates are $2/T$. We assume here a multipath channel with perfect frequency synchronization (no carrier frequency offset or Doppler shift). A time offset can be incorporated in the CIR.

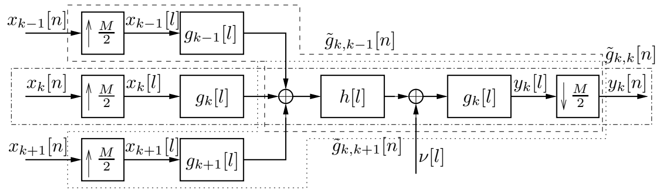

Figure 3. Subchannel model for the FBMC/OQAM system.

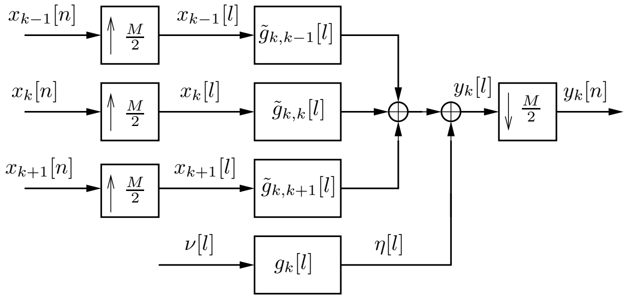

Figure 4. Subcarrier model including broadband channel.

III. Broadband CIR based System Model

The subcarrier model of Fig. 3 can be simplified as shown in Fig. 4 for the purpose of estimating the broadband CIR $h[l]$.

The output $y_k[n]$ contains the received samples at the OQAM symbol rate $\frac{2}{T}$ and is defined as

$$y_k[n] = \sum_{\ell=k-1}^{k+1} \tilde{g}_{k,\ell}[n] * x_\ell[n] + \eta_k[n], \tag{1}$$

where $*$ represents linear convolution, and the $\tilde{g}_{k,\ell}[n]$ is an impulse response of length $L_{\tilde{g}} = \lceil \frac{2L_{\mathrm{P}}+L_h-2}{M/2} \rceil$ that results from the downsampling by $\frac{M}{2}$ of the convolution between the transmit filter $g_\ell[l]$, the receive filter $g_k[l]$ and the frequency selective channel $h[l]$. Moreover, $\eta_k[n]$ is the downsampled narrowband colored noise.

One can stack the coefficients of the impulse response $\tilde{g}_{k,\ell}[n]$ in the vector $\tilde{\mathbf{g}}_{k,\ell} \in \mathbb{C}^{L_{\tilde{g}}}$ and represent it as

$$\tilde{\mathbf{g}}_{k,\ell} = \mathbf{J}_{\mathrm{DS}}^{G} \mathbf{G}_{k,\ell} \mathbf{h} = \bar{\mathbf{G}}_{k,\ell} \mathbf{h}, \tag{2}$$

where $\mathbf{J}_{\mathrm{DS}}^{G}$ is what we call a downsampling matrix, or rows selection matrix, $\mathbf{G}_{k,\ell} \in \mathbb{C}^{(2L_{\mathrm{P}}-1)\times L_h}$ is a convolution matrix generated by the impulse response $(g_k * g_\ell)[l]$, $\bar{\mathbf{G}}_{k,\ell} \in \mathbb{C}^{L_{\tilde{g}}\times L_h}$ contains only some rows of $\mathbf{G}_{k,\ell}$ and $\mathbf{h} \in \mathbb{C}^{L_h}$ is the CIR vector. The downsampling matrix $\mathbf{J}_{\mathrm{DS}}^{G}$ has its j-th row given by $\mathbf{e}_q^T \in \{0,1\}^{(2L_{\mathrm{P}}-1)}$ for $q = (j-1)M/2 + 1$ and $j \in \{1, 2, ..., L_{\tilde{g}}\}$, where $\mathbf{e}_q$ is a unity vector with 1 in the q-th position and 0s elsewhere.

Now, we can stack the samples $y_k[n]$ in an observations vector and, for notational convenience, we drop the time index

$$\begin{aligned}\mathbf{y}_k &= \sum_{\ell=k-1}^{k+1} \mathbf{X}_\ell \tilde{\mathbf{g}}_{k,\ell} + \mathbf{\Gamma}_k \boldsymbol{\nu} = \left(\sum_{\ell=k-1}^{k+1} \mathbf{X}_\ell \bar{\mathbf{G}}_{k,\ell}\right) \mathbf{h} + \mathbf{\Gamma}_k \boldsymbol{\nu}, \\ &= \mathbf{S}_k \mathbf{h} + \boldsymbol{\eta}_k, \end{aligned} \tag{3}$$

where $\mathbf{X}_\ell = \sum_{j=1}^{L_{\tilde{g}}} \mathbf{D}_j \mathbf{x}_\ell \mathbf{e}_j^{\mathrm{T}} \in \mathbb{C}^{L_\mathrm{o} \times L_{\tilde{g}}}$ is a Hankel matrix, $\mathbf{x}_\ell \in \mathbb{C}^{L_x}$ contains the inputs $x_\ell[n]$ and $L_x = L_\mathrm{o} + L_{\tilde{g}} - 1$. Furthermore, $\mathbf{D}_j = [\ \mathbf{0}_{\mathbf{D}1} \quad \mathbf{I}_{L_\mathrm{o}} \quad \mathbf{0}_{\mathbf{D}2}\ ]$ is a matrix that selects L_o rows of $\mathbf{x}_\ell$, where $\mathbf{0}_{\mathbf{D}1} \in \{0\}^{L_\mathrm{o} \times (j-1)}$, $\mathbf{0}_{\mathbf{D}2} \in \{0\}^{L_\mathrm{o} \times (L_{\tilde{g}}-j)}$ and $\mathbf{e}_j \in \{0,1\}^{L_{\tilde{g}}}$ is a unitary vector with 1 in the j-th position and 0s elsewhere. Moreover, we have that $\boldsymbol{\eta}_k = \boldsymbol{\Gamma}_k \boldsymbol{\nu}$, where $\boldsymbol{\Gamma}_k \in \mathbb{C}^{L_\mathrm{o} \times (L_\mathrm{P}+L_\mathrm{o}-1)}$ is the corresponding downsampled version of the convolution matrix generated from the impulse response $g_k[l]$ and $boldsymbol\nu \in \mathbb{C}^{(L_\mathrm{P}+L_\mathrm{o}-1)}$ contains white Gaussian noise samples with zero mean and variance σ_ν^2.

Finally, we stack the M_t vectors with the outputs of the observations subcarriers to obtain

$$\begin{bmatrix} \mathbf{y}_0 \\ \mathbf{y}_1 \\ \vdots \\ \mathbf{y}_{M_\mathrm{t}-1} \end{bmatrix} = \begin{bmatrix} \mathbf{S}_0 \\ \mathbf{S}_1 \\ \vdots \\ \mathbf{S}_{M_\mathrm{t}-1} \end{bmatrix} \mathbf{h} + \begin{bmatrix} \boldsymbol{\Gamma}_0 \\ \boldsymbol{\Gamma}_1 \\ \vdots \\ \boldsymbol{\Gamma}_{M_\mathrm{t}-1} \end{bmatrix} \boldsymbol{\nu},$$
$$\mathbf{y} = \mathbf{S}\mathbf{h} + \boldsymbol{\eta}. \tag{4}$$

It should be noted that we have assumed here that the vectors $\mathbf{y}_k$ collected into $\mathbf{y}$ do not belong to contiguous subcarriers, i.e. the observations are sparsely taken on the subcarrier axis. This means that the training symbols are frequency multiplexed with data symbols.

IV. Maximum Likelihood CIR Estimation

We can see that in (4) the noise $\boldsymbol{\eta}$ is Gaussian distributed with zero mean and covariance matrix $\mathbf{R}_\eta = \sigma_\nu^2 \boldsymbol{\Gamma}\boldsymbol{\Gamma}^{\mathrm{H}} = \mathrm{diag}(\mathbf{R}_{\eta,0}, \mathbf{R}_{\eta,1}, ..., \mathbf{R}_{\eta,M_\mathrm{t}-1})$ and the observation $\mathbf{y}$ given $\mathbf{h}$ is then Gaussian distributed. The maximum likelihood (ML) estimate of $\mathbf{h}$ in this case is given by

$$\begin{aligned} \hat{\mathbf{h}} &= \arg \max_{\mathbf{h} \in \mathbb{C}^{L_h}} p(\mathbf{y}|\mathbf{h}) = \arg \min_{\mathbf{h}} J(\mathbf{h}), \\ &= \left(\mathbf{S}^{\mathrm{H}} \mathbf{R}_\eta^{-1} \mathbf{S}\right)^{-1} \mathbf{S}^{\mathrm{H}} \mathbf{R}_\eta^{-1} \mathbf{y}, \end{aligned} \tag{5}$$

where $J(\mathbf{h}) = (\mathbf{y} - \mathbf{S}\mathbf{h})^{\mathrm{H}} \mathbf{R}_\eta^{-1} (\mathbf{y} - \mathbf{S}\mathbf{h})$ and we assume here that $(\mathbf{S}^{\mathrm{H}} \mathbf{R}_\eta^{-1} \mathbf{S})$ is non-singular. Moreover, the covariance matrix of the estimation error $\boldsymbol{\Delta}\hat{\mathbf{h}} = (\hat{\mathbf{h}} - \mathbf{h})$ of the broadband ML estimator is given by $\mathbf{R}_{\boldsymbol{\Delta}\hat{\mathbf{h}}} = \mathrm{E}\left[\boldsymbol{\Delta}\hat{\mathbf{h}} \boldsymbol{\Delta}\hat{\mathbf{h}}^{\mathrm{H}}\right] = \left(\mathbf{S}^{\mathrm{H}} \mathbf{R}_\eta^{-1} \mathbf{S}\right)^{-1}$. As a consequence, the theoretical MSE of the broadband ML estimator is given by $\epsilon = \frac{\sigma_\nu^2 M_\mathrm{u}}{M} \operatorname{tr}\left\{\mathbf{R}_{\boldsymbol{\Delta}\hat{\mathbf{h}}}\right\}$.

When multicarrier systems like FBMC or CP-OFDM are deployed, the number of subcarriers filled with data and training M_u is smaller than M, in order to allow for upsampling, filtering and D/A conversion. Even if all M_u subcarriers are only filled with training symbols, the estimation of the broadband CIR can only be performed in a fraction of its total frequency response. As a consequence $(\mathbf{S}^{\mathrm{H}} \mathbf{R}_\eta^{-1} \mathbf{S})$ will become ill conditioned or, most probably, singular. The reason is that the portions of the channel frequency response that are not excited cannot and need not be reliably estimated.

To solve this problem we define the downsampled (DS) broadband CIR vector $\mathbf{h}_{\mathrm{DS}} \in \mathbb{C}^{L_{h_{\mathrm{DS}}}}$ that can be estimated in the occupied spectrum. Then we define the linear transformation $\mathbf{h} = \mathbf{A}\mathbf{h}_{\mathrm{DS}}$, that performs a fractionally upsampling of $\mathbf{h}_{\mathrm{DS}}$ by a factor of $L_{\mathrm{frac}} = L_h / L_{h_{\mathrm{DS}}}$, where $L_{h_{\mathrm{DS}}} = \lfloor \frac{M_u}{M} L_h \rfloor$. This operation is performed in three steps: upsampling by a factor of L_h, low-pass filtering and downsampling by a factor $L_{h_{\mathrm{DS}}}$. Mathematically, this can be described by

$$\mathbf{A} = \mathbf{J}_{\mathrm{DS}}^{A} \left[\mathbf{0}_A \quad \mathbf{I}_{L_{h_{\mathrm{DS}}} L_h} \quad \mathbf{0}_A\right] \mathbf{G}_{\mathrm{int}} \mathbf{J}_{\mathrm{US}} \in \mathbb{R}^{L_h \times L_{h_{\mathrm{DS}}}}, \tag{6}$$

where $\mathbf{J}_{\mathrm{DS}}^{A}$ is a downsampling matrix with its ℓ-th row given by $\mathbf{e}_q^T \in \{0,1\}^{(L_{h_{\mathrm{DS}}} L_h)}$ for $q = (\ell-1) L_{h_{\mathrm{DS}}} + 1$ and $\ell \in \{1, 2, ..., L_h\}$, $\mathbf{J}_{\mathrm{US}}$ is an upsampling matrix with its ℓ-th column given by $\mathbf{e}_q \in \{0,1\}^{(L_{h_{\mathrm{DS}}} L_h)}$ for $q = (\ell-1) L_h + 1$ and $\ell \in \{1, 2, ..., L_{h_{\mathrm{DS}}}\}$, $\mathbf{G}_{\mathrm{int}} \in \mathbb{R}^{(L_{h_{\mathrm{DS}}} L_h + 2(d_g-1)) \times (L_{h_{\mathrm{DS}}} L_h)}$ is a convolution matrix obtained from the interpolation filter $\mathbf{g}_{\mathrm{int}} \in \mathbb{R}^{2d_g-1}$, $\mathbf{0}_A \in \{0\}^{(L_{h_{\mathrm{DS}}} L_h) \times (d_g-1)}$. $g_{\mathrm{int}}[n]$ is taken as an FIR approximation of a raised cosine (RC) filter with a sharp roll-off $\alpha = 0.001$, transfer function degree of $L_{g_{\mathrm{int}}} = 10 L_{h_{\mathrm{DS}}} L_h$ and group delay $d_g = 5 L_{h_{\mathrm{DS}}} + 1$.

By substituting $\mathbf{h} = \mathbf{A}\mathbf{h}_{\mathrm{DS}}$ in (4) we can calculate the new ML estimator to obtain

$$\hat{\mathbf{h}}_{\mathrm{DS}} = \left(\mathbf{A}^{\mathrm{H}} \mathbf{S}^{\mathrm{H}} \mathbf{R}_\eta^{-1} \mathbf{S} \mathbf{A}\right)^{-1} \mathbf{A}^{\mathrm{H}} \mathbf{S}^{\mathrm{H}} \mathbf{R}_\eta^{-1} \mathbf{y}, \tag{7}$$

where now $\left(\mathbf{A}^{\mathrm{H}} \mathbf{S}^{\mathrm{H}} \mathbf{R}_\eta^{-1} \mathbf{S} \mathbf{A}\right)$ is neither ill conditioned nor singular and the corresponding MSE is given by

$$\epsilon_{\mathrm{DS}} = \frac{\sigma_\nu^2 M_\mathrm{u}}{M} \operatorname{tr}\left\{\left(\mathbf{A}^{\mathrm{H}} \mathbf{S}^{\mathrm{H}} \mathbf{R}_\eta^{-1} \mathbf{S} \mathbf{A}\right)^{-1}\right\}. \tag{8}$$

A. Spectrally Efficient CIR Estimation

One can see that the model in (3) is dependent on the inputs of 3 adjacent subcarriers and, in addition to that, the number of input symbols to generate $\mathbf{X}_\ell$ is dependent on the prototype length L_P, on the CIR length L_h, and on the number observations L_o collected at the receiver side. Usually, the length of the training should be as short as possible and not necessarily depend on all those factors. Actually, it is usually desired to have short training sequences distributed over the time vs. frequency plane, as for example in LTE standards. In this way one could consider that short training sequences are interpolated in the frequency axis by data subcarriers and data symbols are transmitted immediately before and after the training sequences, without any guard intervals (or empty subcarriers) neither in time nor in frequency.

Let us now define the desired training sequence length $L_\mathrm{t} < L_x$ and the constants $L_{\mathrm{d}1} = \lfloor \frac{L_x - L_\mathrm{t}}{2} \rfloor$ and $L_{\mathrm{d}2} = \lceil \frac{L_x - L_\mathrm{t}}{2} \rceil$. Then, we decompose $\mathbf{X}_\ell = \mathbf{X}_{\mathrm{t},\ell} + \mathbf{X}_{\mathrm{d},\ell}$, where $\mathbf{X}_{\mathrm{t},\ell}$ is generated from the vector $\left[\mathbf{0}_{L_{\mathrm{d}1}}^{\mathrm{T}} \quad \mathbf{x}_{\mathrm{t},\ell}^{\mathrm{T}} \quad \mathbf{0}_{L_{\mathrm{d}1}}^{\mathrm{T}}\right]^{\mathrm{T}} \in \mathbb{C}^{L_x}$ containing training symbols and $\mathbf{X}_{\mathrm{d},\ell}$ is generated from the vector $\left[\mathbf{x}_{\mathrm{d}1,\ell}^{\mathrm{T}} \quad \mathbf{0}_{L_\mathrm{t}}^{\mathrm{T}} \quad \mathbf{x}_{\mathrm{d}2,\ell}^{\mathrm{T}}\right]^{\mathrm{T}} \in \mathbb{C}^{L_x}$ containing data symbols, with $\mathbf{x}_{\mathrm{t},\ell} \in \mathbb{C}^{L_\mathrm{t}}$, $\mathbf{x}_{\mathrm{d}1,\ell} \in \mathbb{C}^{L_{\mathrm{d}1}}$ and $\mathbf{x}_{\mathrm{d}2,\ell} \in \mathbb{C}^{L_{\mathrm{d}2}}$. The reason for this choice of the values of $L_{\mathrm{d}1}$ and $L_{\mathrm{d}2}$ is that the prototype filter IR is symmetric and its energy is concentrated in the coefficients in the middle of the IR.

We further define the following observations vector as a function of two input terms: a training dependent and an interference dependent one

$$\mathbf{y}_k = (\mathbf{S}_k + \mathbf{U}_k)\mathbf{h} + \boldsymbol{\Gamma}_k \boldsymbol{\nu}, \tag{9}$$

where for the model in (3) one can clearly see that $\mathbf{U}_k = \mathbf{0}$. Then, 3 cases can be considered for an spectral efficient channel estimation: (3)

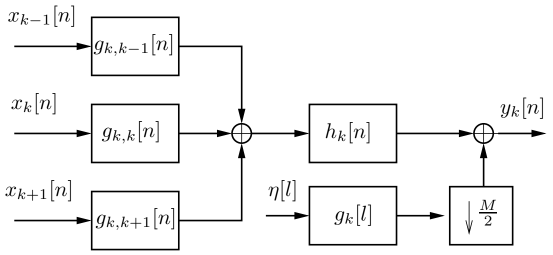

Figure 5. Subcarrier model including the narrowband channels.

- Case 1, ICI limited estimation: $\mathbf{X}_{k+1} = \mathbf{X}_{\mathrm{d},k+1}$ and $\mathbf{X}_{k-1} = \mathbf{X}_{\mathrm{d},k-1}$ contain only data symbols and $\mathbf{X}_k = \mathbf{X}_{\mathrm{t},k}$ is fully filled with training, so that the following definitions hold $\mathbf{S}_k = \mathbf{X}_{\mathrm{t},k}\bar{\mathbf{G}}_{k,k}$ and $\mathbf{U}_k = \mathbf{X}_{\mathrm{d},k-1}\bar{\mathbf{G}}_{k,k-1} + \mathbf{X}_{\mathrm{d},k+1}\bar{\mathbf{G}}_{k,k+1}$.
- Case 2, ISI limited estimation: We use the decomposition of $\mathbf{X}_\ell$ to get the matrices $\mathbf{S}_k = \sum_{\ell=k-1}^{k+1} \mathbf{X}_{\mathrm{t},\ell}\bar{\mathbf{G}}_{k,\ell}$ and $\mathbf{U}_k = \sum_{\ell=k-1}^{k+1} \mathbf{X}_{\mathrm{d},\ell}\bar{\mathbf{G}}_{k,\ell}$.
- Case 3, ICI and ISI limited estimation: We decompose only $\mathbf{X}_k$ to get the matrices $\mathbf{S}_k = \mathbf{X}_{\mathrm{t},k}\bar{\mathbf{G}}_{k,k}$ and $\mathbf{U}_k = \mathbf{X}_{\mathrm{d},k}\bar{\mathbf{G}}_{k,k} + \mathbf{X}_{\mathrm{d},k-1}\bar{\mathbf{G}}_{k,k-1} + \mathbf{X}_{\mathrm{d},k+1}\bar{\mathbf{G}}_{k,k+1}$.

Similar to (4) the observations can be stacked to get

$$\mathbf{y} = (\mathbf{S} + \mathbf{U})\mathbf{h} + \boldsymbol{\eta}. \tag{10}$$

The estimator in (7) can then be employed and, for the moment, the interference term $\mathbf{U}\mathbf{h}$ is just ignored. In [4] and [5] we have proposed methods to iteratively estimate the $\mathbf{h}$ and $\mathbf{U}$ for the Case 1 and we have shown that the estimation quality can be significantly improved. Extensions for the cases 2 and 3 will be left for a future publication.

V. Narrowband CIRs based System Model

The block diagram in Fig. 3 can be redraw in order to obtain a model where the received signal in each subcarrier is a function of a narrowband channel. This model is represented in Fig. 5. Of course that one can only estimate the narrowband channels $h_k[n]$ in the subcarriers that are filled with training sequences and the broadband channel can be obtained by a interpolation, for example.

In a similar way as we did for the broadband channel, for the narrowband channel estimation we can write

$$\begin{aligned}\mathbf{y}_k &= \left(\sum_{\ell=k-1}^{k+1} \mathbf{X}'_\ell \bar{\mathbf{G}}'_{k,\ell}\right)\mathbf{h}_k + \boldsymbol{\Gamma}_k\boldsymbol{\nu}, \\ &= \mathbf{S}'_k\mathbf{h}_k + \boldsymbol{\Gamma}_k\boldsymbol{\nu},\end{aligned} \tag{11}$$

where now $\mathbf{X}'_\ell \in \mathbb{C}^{L_\mathrm{o}\times L_{\bar{g}'}}$, $\bar{\mathbf{G}}'_{k,\ell} \in \mathbb{C}^{L_{\bar{g}'}\times L_{h_k}}$, $\mathbf{h}_k \in \mathbb{C}^{L_{h_k}}$, with $L_{\bar{g}'} = L_{h_k} + L_{\bar{g}'} - 1$ and $L_{\bar{g}'} = \lceil \frac{2L_\mathrm{p}-1}{M/2} \rceil$. One can see that the length of the input vectors L_x and $L_{x'}$ are only equal for a very special combination of parameters, including the IR length of the narrowband channels, that in addition to the number of observations have a strong influence in the performance of the estimator.

The narrowband channel observed in each subcarrier can calculated from the broadband channel by the transformation $\mathbf{h}_k = \mathbf{B}_k\mathbf{h}$. Thereby, the following definition holds

$$\mathbf{B}_k = \begin{bmatrix}\mathbf{I}_{L_{h_k}} & \mathbf{0}_{B1}\end{bmatrix}\mathbf{F}^{\mathrm{H}}_{L_{h_k}M_i}\begin{bmatrix}\mathbf{0}_{B2} & \mathbf{I}_{L_{h_k}M_i} & \mathbf{0}_{B3}\end{bmatrix}\mathbf{F}_{M_f}\begin{bmatrix}\mathbf{I}_{L_h} \\ \mathbf{0}_{B4}\end{bmatrix},$$

with $\mathbf{F}_{M_f}$ being an M_f-DFT matrix, $M_f = ML_{h_k}M_i$, $\mathbf{0}_{B1} \in \{0\}^{L_{h_k}\times(L_{h_k}(M_i-1))}$, $\mathbf{0}_{B2} \in \{0\}^{(L_{h_k}M_i)\times(kL_{h_k}M_i)}$, $\mathbf{0}_{B3} \in \{0\}^{(L_{h_k}M_i)\times((M-1-k)L_{h_k}M_i)}$, $\mathbf{0}_{B4} \in \{0\}^{(M_f-L_h)\times L_h}$, M_i is a resolution factor for the calculation's resolution of the $\mathbf{h}_k$s.

As a consequence we can rewrite (11) as follows

$$\mathbf{y}_k = \mathbf{S}'_k\mathbf{B}_k\mathbf{h} + \boldsymbol{\Gamma}_k\boldsymbol{\nu}, \tag{12}$$

and similar to (4) we can write $\mathbf{y} = \mathbf{S}'\mathbf{h} + \boldsymbol{\eta}$, with $\mathbf{S}'^{\mathrm{T}} = \begin{bmatrix}\mathbf{B}_0^{\mathrm{T}}\mathbf{S}_0'^{\mathrm{T}} & \mathbf{B}_1^{\mathrm{T}}\mathbf{S}_1'^{\mathrm{T}} & .. & \mathbf{B}_{M_\mathrm{t}-1}^{\mathrm{T}}\mathbf{S}_{M_\mathrm{t}-1}'^{\mathrm{T}}\end{bmatrix}^{\mathrm{T}}$. Furthermore, the same ML channel estimation expression as the one used for the broadband CIR based model in (7) can be applied, if we employ the corresponding matrices defined above.

Regarding the spectrally efficient channel estimation, the same three cases as in the broadband CIR based model exist and again we just have to employ the corresponding matrices.

It is worth noting that besides the different definitions of the matrices used for the channel estimation, for the narrowband CIR based model there is one more parameter to be determined, namely the narrowband channel length L_{h_k}

VI. Simulation Results

For the performance evaluations, the parameters were $M = 256$, $M_\mathrm{u} = 156$, $K = 4$ and the prototype was an RRC filter with roll-off one. The total signal bandwidth is 12.6 MHz and the sampling rate is $M/T = 15.36$ MHz, giving a subcarrier bandwidth of 60 kHz and a symbol duration of $T = 16.67$ μs. The channel model was the ITU-Vehicular A without mobility. The CIR duration is $L_h = 36$ samples.

The observations were taken from every 4-th subcarrier, resulting in $M_\mathrm{t} = 39$ observations subcarriers. For case 1 and 3, only those 39 are filled with training. 117 subcarriers are filled with training for the interference free estimation and for the case 2. All the other subcarriers in all cases are filled with random QPSK data symbols. Moreover, we have used random QPSK training symbols. The normalized MSE (NMSE) $\bar{\epsilon} = \frac{\mathrm{E}[\epsilon_{\mathrm{DS}}]}{\mathrm{E}[||\mathbf{h}_{\mathrm{DS}}||]}$ of the channel estimation was averaged over 100 channel realizations, each was also averaged over 10 training sequences and, for each training, averaged over 10 noise realizations.

In Fig. 6 we show simulation results for both broadband and narrowband model for $L_\mathrm{o} = 4$ observations. For cases 2 and 3 the OQAM training length is $L_\mathrm{t} = 4$, what is equivalent to two QAM symbols. For the narrowband model we have used $L_{h_k} = 3$ for each subcarrier. We can see that the interference worses the performance of both channel estimators as expected. The use of different models seems to make no difference in the results for this set of parameters.

One extreme example is shown in Fig. 7, where the main difference is for cases 2 and 3 with OQAM training length is now $L_\mathrm{t} = 2$, what is equivalent to one QAM symbols in

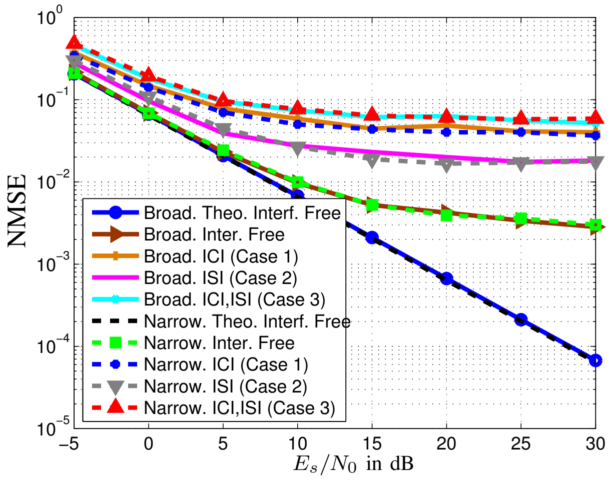

Figure 6. MSE as a function of E_s/N_0 for $L_\mathrm{t} = 4$.

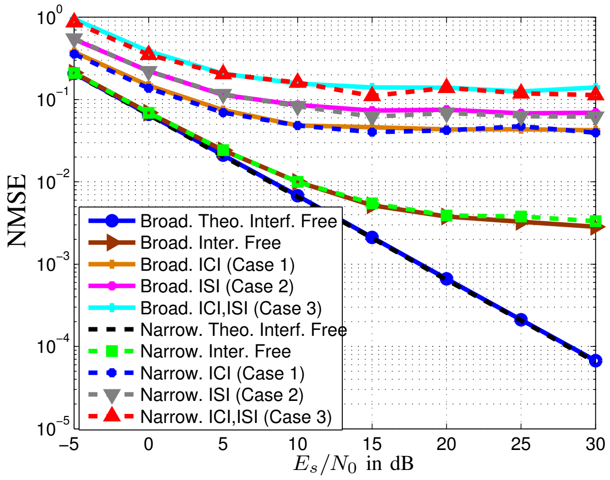

Figure 7. MSE as a function of E_s/N_0 for $L_\mathrm{t} = 2$.

each training subcarrier. Here the training length is minimal and, for the three cases, one can see that both broadband and narrowband based models show the same performance when the interference is ignored.

To better illustrate the effect of longer training sequences we show in Fig. 8 an example where $L_\mathrm{t} = 6$, i.e. 3 QAM symbols long. It is possible to see that the performances for cases 1 and 3 get very close to each other, because the ISI in this case becomes negligible compared to the ICI, that dominates also over the noise for a wide range of E_s/N_0. It is also possible to see that the case 2 gets very close to the interference free case for the broadband based model and for the narrowband not that much. The reason for that is the length of the necessary interference free training length for this model. If we extend the training to $L_\mathrm{t} = 8$ the result becomes identical to the interference free one for the same parameters.

VII. Conclusions

In this contribution we have presented a parallel between two models for the channel estimation in a prominent multicarrier system, the OQAM/FBMC system. We have called them broadband and narrowband based models. In both cases the impulse response of the propagation channel is estimated for the whole transmission bandwidth. In addition to that, we have considered three possibilities for a spectrally efficient estimation. In the three cases the existing interference is composed by different parts that are related to the adjacent subcarriers and to the subcarrier being observed. The simulation results show that very short training could be used: not more than three QAM symbols. But if the adjacent subcarriers are filled with data, a dramatic loss in performance can be observed.

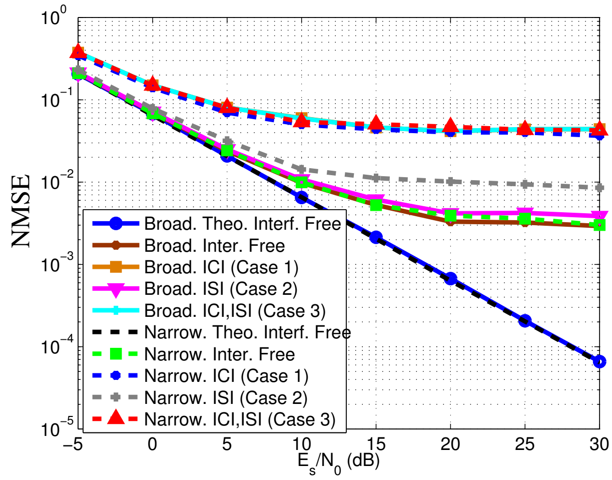

Figure 8. MSE as a function of E_s/N_0 for $L_\mathrm{t} = 6$.

Acknowledgment

The authors acknowledge the financial support by the EU FP7-ICT project EMPhAtiC (http://www.ictemphatic.eu) under grant agreement no. 318362.

References

[1] B. Saltzberg, "Performance of an efficient parallel data transmission system," *IEEE Trans. Comm. Technology*, vol. COM-15, no. 6, pp. 805–811, Dec. 1967.

[2] E. Kofidis, "Preamble-based channel estimation in OFDM/OQAM systems: A time-domain approach," *arXiv*, June 2013.

[3] L. Baltar, M. Newinger, and J. Nossek, "Structured subchannel impulse response estimation for filter bank based multicarrier systems," in *Wireless Communication Systems (ISWCS), 2012 International Symposium on*, 2012, pp. 191–195.

[4] L. Baltar, A. Mezghani, and J. Nossek, "EM based per-subcarrier ML channel estimation for filter bank multicarrier systems," in *Proc. of the 10-th Int. Symposium on Wireless Comm. Systems ISWCS 2013*. [Online]. Available: http://ieeexplore.ieee.org/stamp/stamp.jsp?arnumber=6629690

[5] L. Baltar, T. Laas, M. Newinger, A. Mezghani, and J. Nossek, "Enhancing spectral efficiency in advanced multicarrier techniques: A challenge," in *Proceedings of the 22nd European Signal Processing Conference (EUSIPCO-2014)*, Lisbon, Portugal, September 2014.

[6] D. Waldhauser, L. Baltar, and J. Nossek, "MMSE subcarrier equalization for filter bank based multicarrier systems," in *Proc. IEEE 9th Workshop Signal Proc. Advances in Wireless Comm. SPAWC 2008*.

[7] T. Karp and N. Fliege, "Modified DFT filter banks with perfect reconstruction," *IEEE Trans. on Circuits and Systems II: Analog and Digital Signal Proc.*, vol. 46, no. 11, pp. 1404–1414, Nov. 1999.